Bulletin of the Seismological Society of America, Vol. 106, No. 1, pp. 316–320, February 2016, doi: 10.1785/0120150229

*Short Note*

# Determining Generic Velocity and Density Models for Crustal Amplification Calculations, with an Update of the Boore and Joyner (1997) Generic Site Amplification for $\bar{V}_S(Z) = 760$ m/s

by David M. Boore

**Abstract** This short note contains two contributions related to deriving depth-dependent velocity and density models for use in computing generic crustal amplifications. The first contribution is a method for interpolating two velocity profiles to obtain a third profile with a time-averaged velocity $\bar{V}(Z)$ to depth $Z$ that is equal to a specified value (e.g., for shear-wave velocity $V_S$, $\bar{V}_S(Z) = 760$ m/s for $Z = 30$ m, in which the subscript $S$ has been added to indicate that the average is for shear-wave velocities). The second contribution is a procedure for obtaining densities from $V_S$. The first contribution is used to extend and revise the Boore and Joyner (1997) generic rock $V_S$ model, for which $\bar{V}_S(30\text{ m}) = 618$ m/s, to a model with the more common $\bar{V}_S(30\text{ m}) = 760$ m/s. This new model is then used with the densities from the second contribution to compute crustal amplifications for a generic site with $\bar{V}_S(30\text{ m}) = 760$ m/s.

## Introduction

Even though the generic rock velocity model of Boore and Joyner (1997; hereafter referred to as BJ97) with $\bar{V}_S(30\text{ m}) = 618$ m/s (hereafter referred to as BJ97gr) has been widely used to compute crustal amplifications, it is desirable to have a shear-wave velocity model for which $\bar{V}_S(30\text{ m}) = 760$ m/s, because this is the reference condition used in a number of applications and studies (e.g., the U.S. Geological Survey National Seismic Hazard Maps; Peterson *et al.*, 2014). Because the difference between 618 and 760 m/s is so small, I decided to use an interpolation of the BJ97 generic rock and generic very hard rock velocity models to obtain the desired velocity model, which I call BJ97gr760. The interpolation method has not been published before. In addition, calculations of crustal amplifications require a density model as a function of depth. This article documents a modification to the procedure used in Boore and Joyner (1997) to obtain densities from $V_S$. The interpolation procedure and the density–$V_S$ relation were used to obtain crustal amplifications for the BJ97gr760 model.

## Interpolating Two Velocity Models to Obtain a Model with a Specified $\bar{V}_S(Z)$

The idea of interpolating two models to obtain a third one with a specified time-averaged velocity to a specified depth $Z$ was taken from Cotton *et al.* (2006) but with a modification guaranteeing that the condition on the average velocity is satisfied. The definition of the time-averaged velocity to any depth $Z$ is given by

$$\bar{V}(Z) = Z / \int_0^Z \frac{1}{V(\xi)} \mathrm{d}\xi, \tag{1}$$

in which the overbar indicates an average quantity. I do not include a subscript $S$ on $\bar{V}$, indicating $V_S$, because the formulation works for any type of velocity profile. The notation for the average velocity to depth $Z$ in equation (1) is used for simplicity in later equations; the usual notation of $V_{S30}$ (e.g., Ancheta *et al.*, 2014) is equivalent to $\bar{V}(30\text{ m})$, in which the velocity function in the integral in equation (1) is $V_S$, averaged from the surface to 30 m.

It is convenient to work with seismic slowness, which has a number of advantages over seismic velocity in site response studies, as discussed, for example, by Brown *et al.* (2002) and Boore and Thompson (2007). The slowness and velocity are related to one another by the equation

$$S(z) = \frac{1}{V(z)}. \tag{2}$$

In terms of slowness, the equivalent of equation (1) is

$$\bar{S}(Z) = \frac{1}{Z} \int_0^Z S(\xi) \mathrm{d}\xi, \tag{3}$$

and

$$\bar{V}(Z) = \frac{1}{\bar{S}(Z)}. \tag{4}$$

Now assume that two slowness models are available, $S_1(z)$ and $S_2(z)$, and that a third profile is obtained from a linear combination of these two profiles, using the following equation:

$$S(z) = (1-\beta)S_1(z) + \beta S_2(z). \tag{5}$$

The coefficient $\beta$ can be obtained by requiring that the average slowness to depth $Z$, $\bar{S}(Z)$, equals a desired value $\bar{S}_D$. With this condition, equations (3) and (5) can be combined to give

$$\bar{S}_D = (1-\beta)\bar{S}_1(Z) + \beta\bar{S}_2(Z), \tag{6}$$

and this can be solved for $\beta$:

$$\beta = \frac{\bar{S}_D - \bar{S}_1(Z)}{\bar{S}_2(Z) - \bar{S}_1(Z)}. \tag{7}$$

$S(z)$ can take any value below depth $Z$ without affecting the constraint that $\bar{S}(Z) = \bar{S}_D$. The simplest assumption is that equation (5) be used for all depths greater than $Z$. Because $S(z)$ usually becomes smaller with increasing depth and thus has proportionally less impact on site amplifications than does $S(z)$ at shallow depths, differences in slowness profiles at deeper depths are less important than at shallow depths.

The procedure above differs from that of Cotton *et al.* (2006) in that their interpolation is in terms of the logarithm of velocity, and they apply the interpolation to a small subset of anchor depths, with a power-law function for the velocities at depths between the anchor depths.

## Obtaining Densities from Shear-Wave Velocities

Calculations of site amplification require both velocity and density as a function of depth. Although the velocity model is usually specified, seldom is the density model given. I present here a procedure for obtaining densities from $V_S$. This procedure has evolved from the one given by equation (3) in BJ97 (and used for calculations done by me for Frankel *et al.*, 1996), for which the minimum density was 2.5 $\mathrm{g/cm^3}$. I realized that this was too high; and, in unpublished notes made available on my website, I revised the procedure such that the minimum density was 1.93 $\mathrm{g/cm^3}$. After reviewing recent collections of velocity and density data, I made another revision for which the minimum density is now 1.0 $\mathrm{g/cm^3}$. This procedure relies heavily on the Brocher (2005) summary of several relations between densities ($\rho$) and seismic-wave velocities, as well as between compressional-wave velocity ($V_P$) and $V_S$. Those relations, however, are only valid for $V_P > 1.5$ km/s and $V_S > \approx 0.3$ km/s. After reviewing data sets for low values of $V_S$ from P. Anbazhagan (written comm., 2014 and 2015), P. Anbazhagan *et al.* (unpublished manuscript, 2015), Inazaki (2006), and a number of publications from P. Mayne (in particular, Mayne, 2001, and Mayne *et al.*, 2002), I adjusted the coefficients of a function used by Mayne *et al.* (1999) such that a reasonable subjective fit to the data was achieved and the function smoothly joined the relations in Brocher (2005) for $V_S > 0.30$ km/s. The procedure for obtaining the density ($\rho$) from the $V_S$ is summarized here (additional details are in unpublished notes referenced in Data and Resources). The units of velocity are kilometers per second, and those of density are grams per cubic centimeter.

For $V_S < 0.30$ km/s:

$$\rho = 1 + \frac{1.53V_S^{0.85}}{0.35 + 1.889V_S^{1.7}}. \tag{8}$$

For 0.30 km/s $< V_S <$ 3.55 km/s:

$$\rho = 1.74V_P^{0.25}, \tag{9}$$

(Gardner *et al.*, 1974), in which

$$V_P = 0.9409 + 2.0947V_S - 0.8206V_S^2 + 0.2683V_S^3 - 0.0251V_S^4, \tag{10}$$

(equation 9 of Brocher, 2005).

For 3.55 km/s $\le V_S$:

$$\rho = 1.6612V_P - 0.4721V_P^2 + 0.0671V_P^3 - 0.0043V_P^4 + 0.000106V_P^5 \tag{11}$$

(equation 1 of Brocher, 2005), in which equation (10) is used to obtain $V_P$ given $V_S$.

Figure 1 shows the relation between density and $V_S$ obtained from the above procedure, superimposed on a collection of measurements from Mayne (2001; also in Mayne *et al.*, 2002). Assuming homoskedasticity, the standard deviation of the residuals of the data shown in Figure 1 about the curve is 0.13 $\mathrm{g/cm^3}$. (Note that in this article, I use both kilometers and meters and kilometers per second and meters per second as the units for depth and velocity, respectively, according to the depth range under consideration.)

## Application of Interpolation Procedure and Velocity–Density Relations: Crustal Amplifications for BJ97gr760 Velocity Model

I used the above procedure to obtain the BJ97gr760 velocity model and corresponding densities. The BJ97gr760 model was derived by interpolation of the Boore and Joyner (1997) generic rock (BJ97gr) and generic very hard rock (BJ97gvhr) models; these models and their values of $\bar{V}_S$(30 m) are shown in Figure 2. A decimated version of the BJ97gr760 velocities and corresponding densities are given in Table 1. $\bar{V}_S$(30 m) = 759 m/s for this model (and 760 m/s for the undecimated version; see Table 1). In comparison, the Cotton *et al.* (2006) procedure gives $\bar{V}_S$(30 m) = 706 m/s, using their an-

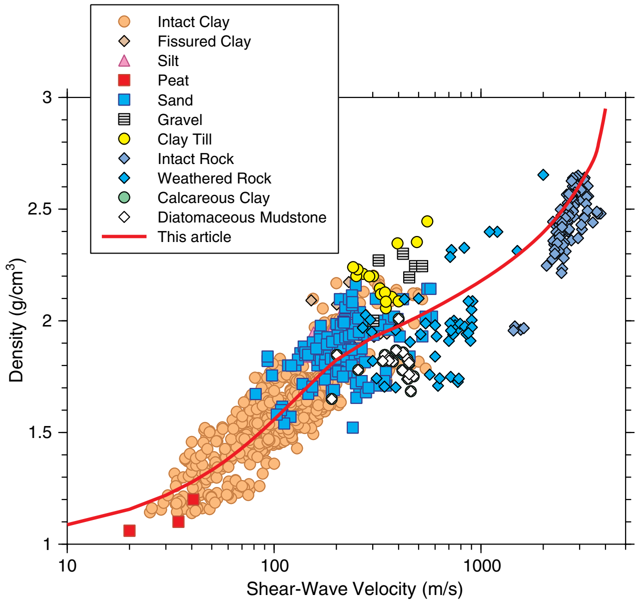


**Figure 1.** The relation between density and shear-wave velocity ($V_S$) proposed in this article, compared with data from Mayne (2001; also in Mayne *et al.*, 2002). More data than shown here were used to establish the curve for larger velocities; see Gardner *et al.* (1974) and Brocher (2005). The color version of this figure is available only in the electronic edition.

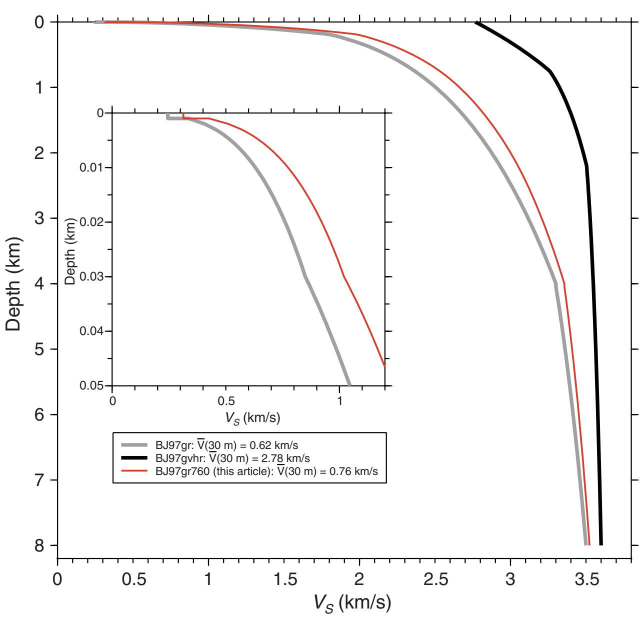


**Figure 2.** $V_S$ as a function of depth for the Boore and Joyner (1997; BJ97) generic rock (BJ97gr) and generic very hard rock (BJ97gvhr) models, and the interpolation of those two models such that $\bar{V}_S(30\text{ m}) = 0.76$ km/s (BJ97gr760). The color version of this figure is available only in the electronic edition.

chor depths of 1 and 30 m and $\bar{V}_S(30\text{ m}) = 764$ m/s if the anchor depths are at 1 m increments.

Following BJ97, the crustal amplifications for a site with $\bar{V}_S(30\text{ m}) = 760$ m/s, relative to material with a density and $V_S$ of 2.72 g/cm$^3$ and 3.5 km/s, respectively, were computed

Table 1
A Shear-Wave Velocity Model Corresponding to the BJ97gr760 Derived in This Article and the Associated Density Model

| $Z$ (km) | $V_S$ (km/s) | Density (g/cm$^3$) |
|---|---|---|
| 0.000 | 0.314 | 1.934 |
| 0.001 | 0.314 | 1.934 |
| 0.001 | 0.427 | 1.989 |
| 0.002 | 0.512 | 2.024 |
| 0.003 | 0.569 | 2.046 |
| 0.005 | 0.649 | 2.075 |
| 0.008 | 0.731 | 2.103 |
| 0.011 | 0.793 | 2.122 |
| 0.014 | 0.843 | 2.136 |
| 0.018 | 0.898 | 2.152 |
| 0.022 | 0.944 | 2.164 |
| 0.030 | 1.020 | 2.184 |
| 0.044 | 1.176 | 2.222 |
| 0.064 | 1.348 | 2.260 |
| 0.082 | 1.474 | 2.287 |
| 0.102 | 1.594 | 2.312 |
| 0.126 | 1.718 | 2.338 |
| 0.150 | 1.826 | 2.360 |
| 0.190 | 1.984 | 2.392 |
| 0.250 | 2.080 | 2.412 |
| 0.300 | 2.147 | 2.426 |
| 0.450 | 2.308 | 2.459 |
| 0.550 | 2.393 | 2.477 |
| 0.650 | 2.467 | 2.493 |
| 0.800 | 2.561 | 2.513 |
| 0.900 | 2.614 | 2.524 |
| 1.000 | 2.663 | 2.535 |
| 1.450 | 2.839 | 2.573 |
| 2.050 | 3.014 | 2.612 |
| 2.400 | 3.094 | 2.629 |
| 2.850 | 3.180 | 2.648 |
| 3.400 | 3.271 | 2.668 |
| 4.000 | 3.357 | 2.687 |
| 5.200 | 3.418 | 2.701 |
| 6.650 | 3.478 | 2.714 |
| 7.850 | 3.519 | 2.723 |

The continuous profiles are represented by line segments connecting the tabulated values. The BJ97gr760 model was derived from interpolation of the BJ97gr and the BJ97gvhr models sampled at 1-m-depth increments to 30 m, with increasing spacing at greater depths, for a total of 273 depths. The model in this table is a decimated version of the BJ97gr760 model, which uses only 36 depth points. The $\bar{V}_S(30\text{ m})$ values are 760 and 759 m/s for the BJ97gr760 models and the one given in this table, respectively.

using the square-root-impedance method (Boore, 2013) for the BJ97gr760 model, and associated densities are given in Table 1. The results are given in Table 2 and are plotted in Figure 3, along with the amplifications for the BJ97gr velocity model (and densities from the procedure given in this article). As is usual for amplifications computed using the square-root-impedance method (see Boore, 2013), attenuation is incorporated by applying the operator $\exp(-\pi\kappa_0 f)$ to the square-root-impedance amplifications, in which $f$ is frequency and $\kappa_0$ is the attenuation parameter. The consequence of doing so is shown in Figure 3 for a wide range of $\kappa_0$.

The variability of the density data about the mean curve used to derive the densities used in the amplifications intro-

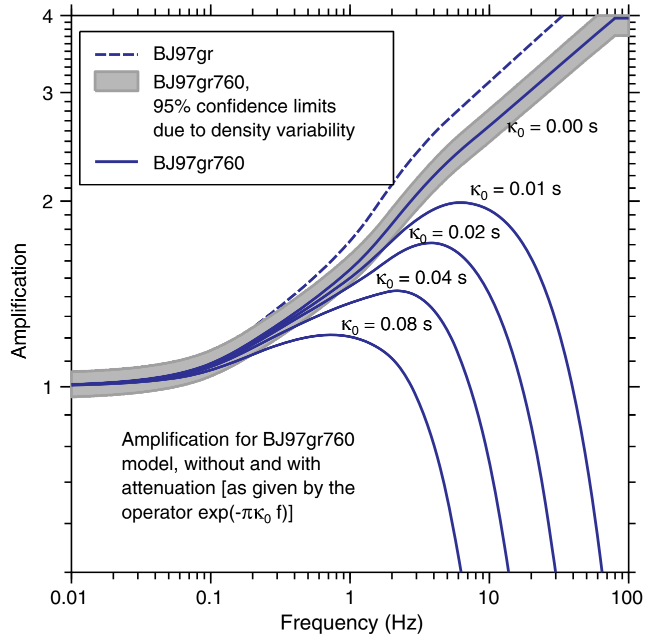


**Figure 3.** The combined effect of the amplification for the BJ97gr760 model in Table 1 and the attenuation given by $\exp(-\pi\kappa_0 f)$. The shaded band around the $\kappa_0 = 0.0$ s curve indicates the 95% confidence limits due to the uncertainty in the density–velocity relation (see text). For comparison, the dashed line is the amplification for the BJ97gr velocity model, using the densities computed using the procedure in this article. This figure is equivalent to figure 8 in Boore and Joyner (1997). The color version of this figure is available only in the electronic edition.

duces uncertainty in the amplifications. To estimate the impact of this density variability, I did a simulation study in which the amplifications were computed for a large number of densities chosen from a normal distribution with a standard deviation of 0.13 $g/cm^3$ (the value for the data shown in Fig. 1) and a mean equal to that used in the amplification calculation at each frequency. The 95% confidence limits are shown by the gray band in Figure 3. It is clear that the variability in the density–velocity relation only introduces a small uncertainty in the computed amplifications. Because I am considering a specific velocity profile, there is no uncertainty due to the velocity model; some idea of the variability in amplification due to the velocity model is in Campbell and Boore (2016), who show amplifications for a number of models for which $\bar{V}_S(30\ \text{m}) = 760$ m/s.

## Discussion and Conclusions

The procedure given here for obtaining a velocity model from interpolation of two velocity models and for obtaining density from $V_S$ are updates of procedures given in unpublished notes. As such, the contributions in this article constitute a formal publication of material used in a number of studies. In addition, the amplifications for the BJ97gr760 model are given as an alternative to the widely used BJ97gr amplifications (as given in table 4 of Boore and Thompson, 2015).

Table 2
Crustal Amplification Model with No Attenuation ($\kappa_0 = 0.0$ s)

| Frequency (Hz) | BJ97gr760 Model |
|---|---|
| 0.010 | 1.00 |
| 0.015 | 1.01 |
| 0.021 | 1.02 |
| 0.031 | 1.02 |
| 0.045 | 1.04 |
| 0.065 | 1.06 |
| 0.095 | 1.09 |
| 0.138 | 1.13 |
| 0.200 | 1.18 |
| 0.291 | 1.25 |
| 0.423 | 1.32 |
| 0.615 | 1.41 |
| 0.894 | 1.51 |
| 1.301 | 1.64 |
| 1.892 | 1.80 |
| 2.751 | 1.99 |
| 4.000 | 2.18 |
| 5.817 | 2.38 |
| 8.459 | 2.56 |
| 12.301 | 2.75 |
| 17.889 | 2.95 |
| 26.014 | 3.17 |
| 37.830 | 3.42 |
| 55.012 | 3.68 |
| 80.000 | 3.96 |

The amplifications are for the densities and shear-wave velocities ($V_S$) given in Table 1 and are relative to a model with a reference velocity and density of 3.5 km/s and 2.72 $g/cm^3$, respectively.

## Data and Resources

The figures were prepared using CoPlot (www.cohort.com, last accessed October 2015). The latest version of the site amplification program (*site_amp_batch*) used for the simulations is part of the SMSIM software package (Boore, 2005), which can be obtained from the online software link on http://www.daveboore.com (last accessed October 2015). More discussion regarding the interpolation of two velocity profiles to yield a third profile with a specified $\bar{V}(Z)$ is in daves_notes_on_interpolating_two_given_velocity_profiles_to_obtain_a_velocity_profile_with_specified_vz.v2.0.pdf, and more information about the relation between density and velocity is given in daves_notes_on_relating_density_to_velocity_v3.0.pdf, both of which are available at http://www.daveboore.com/daves_notes.html (last accessed October 2015). The unpublished manuscript by P. Anbazhagan, U. Anjali, S. Moustafa, and N. Al-Arifi, “Correlation of densities with shear wave velocities and SPT $N$ values”, has been submitted to *J. Geophys. Eng*.

## Acknowledgments

The author would like to thank Ken Campbell for the suggestion that the Boore and Joyner (1997) generic rock amplifications be extended to a model for which $\bar{V}_S(30\ \text{m}) = 760$ m/s, P. Anbazhagan for data and information in advance of publication, Paul Mayne for data and various figures and publications, and Sinan Akkar, Ken Campbell, Eric Thompson, and an anonymous reviewer for useful comments. Any use of trade, firm, or product names is for descriptive purposes only and does not imply endorsement by the U.S. Government.

## References

Ancheta, T. D., R. B. Darragh, J. P. Stewart, E. Seyhan, W. J. Silva, B. S. J. Chiou, K. E. Wooddell, R. W. Graves, A. R. Kottke, D. M. Boore, *et al.* (2014). NGA-West2 database, *Earthq. Spectra* **30,** 989–1005.

Boore, D. M. (2005). SMSIM—Fortran programs for simulating ground motions from earthquakes: Version 2.3—A revision of OFR 96-80-A, *U.S. Geol. Surv. Open-File Rept. 00-509*, revised on 15 August 2005, 55 pp.

Boore, D. M. (2013). The uses and limitations of the square-root impedance method for computing site amplification, *Bull. Seismol. Soc. Am.* **103,** 2356–2368.

Boore, D. M., and W. B. Joyner (1997). Site amplifications for generic rock sites, *Bull. Seismol. Soc. Am.* **87,** 327–341.

Boore, D. M., and E. M. Thompson (2007). On using surface-source downhole-receiver logging to determine seismic slownesses, *Soil Dynam. Earthq. Eng.* **27,** 971–985.

Boore, D. M., and E. M. Thompson (2015). Revisions to some parameters used in stochastic-method simulations of ground motion, *Bull. Seismol. Soc. Am.* **105,** 1029–1041.

Brocher, T. M. (2005). Empirical relations between elastic wavespeeds and density in the Earth's crust, *Bull. Seismol. Soc. Am.* **95,** 2081–2092.

Brown, L. T., D. M. Boore, and K. H. Stokoe (2002). Comparison of shear-wave slowness profiles at ten strong-motion sites from non-invasive SASW measurements and measurements made in boreholes, *Bull. Seismol. Soc. Am.* **92,** 3116–3133.

Campbell, K. W., and D. M. Boore (2016). Evaluation of five generic NEHRP B/C crustal 184 amplification models for active crustal regions, *Bull. Seismol. Soc. Am.* **106,** doi: 10.1785/0120150242.

Cotton, F., F. Scherbaum, J. J. Bommer, and H. Bungum (2006). Criteria for selecting and adjusting ground-motion models for specific target regions: Application to central Europe and rock sites, *J. Seismol.* **10,** 137–156.

Frankel, A., C. Mueller, T. Barnhard, D. Perkins, E. Leyendecker, N. Dickman, S. Hanson, and M. Hopper (1996). National Seismic Hazard Maps: Documentation June 1996, *U.S. Geol. Surv. Open-File Rept. 96-532*, 69 pp.

Gardner, G. H. F., L. W. Gardner, and A. R. Gregory (1974). Formation velocity and density—The diagnostic basics for stratigraphic traps, *Geophysics* **39,** 770–780.

Inazaki, T. (2006). Relationship between S-wave velocities and geotechnical properties of alluvial sediments, *Proc. of the 19th Annual Symposium on Application of Geophysics to Engineering and Environmental Problems (SAGEEP2006) (CD-ROM)*, 1296–1303, doi: 10.4133/1.2923587.

Mayne, P. W. (2001). Stress-strain-strength-flow parameters from enhanced in-situ tests, in P. P. Rahardjho and T. Lunne (Editors), *Proc. of the International Conference on In-Situ Measurement of Soil Properties & Case Histories (In-Situ 2001)*, Bali, Indonesia, 21–24 May 2001, 27–47.

Mayne, P. W., B. Christopher, R. Berg, and J. DeJong (2002). *Subsurface Investigations—Geotechnical Site Characterization*, Publication Number FHWA-NHI-01-031, National Highway Institute, Federal Highway Administration, Washington, D.C., 301 pp.

Mayne, P. W., J. A. Schneider, and G. K. Martin (1999). Small- and high-strain soil properties from seismic flat dilatometer tests, in *Pre-Failure Deformation Characteristics of Geomaterials*, M. Jamiolkowski, R. Lancellotta, and D. LoPresti (Editors), Vol. 1, Rotterdam, The Netherlands, 419–426.

Petersen, M. D., M. P. Moschetti, P. M. Powers, C. S. Mueller, K. M. Haller, A. D. Frankel, Y. Zeng, S. Rezaeian, S. C. Harmsen, O. S. Boyd, *et al.* (2014). Documentation for the 2014 update of the United States National Seismic Hazard Maps, *U.S. Geol. Surv. Open-File Rept. 2014–1091*, 243 pp.

U.S. Geological Survey
MS 977
345 Middlefield Road
Menlo Park, California 94025
boore@usgs.gov

Manuscript received 5 November 2015;
Published Online 29 December 2016